Anomalous Minimum in the Shear Viscosity of a Fermi Gas

E. Elliott,[1,2] J. A. Joseph,[1] and J. E. Thomas[1]
[1]Department of Physics, North Carolina State University, Raleigh, North Carolina 27695, USA
[2]Department of Physics, Duke University, Durham, North Carolina 27708, USA
(Received 6 November 2013; revised manuscript received 21 April 2014; published 10 July 2014)

We measure the static shear viscosity η in a two-component Fermi gas near a broad collisional (Feshbach) resonance, as a function of interaction strength and energy. We find that η has both a quadratic and a linear dependence on the interaction strength $1/(k_{FI}a)$, where a is the s-wave scattering length and k_{FI} is the Fermi wave vector for an ideal gas at the trap center. For energies above the superfluid transition, the minimum in η as a function of interaction strength is significantly shifted toward the BEC side of resonance, to $1/(k_{FI}a) \simeq 0.25$.

DOI: 10.1103/PhysRevLett.113.020406 PACS numbers: 03.75.Ss

Ultracold Fermi gases provide a unique model for studying the properties of strongly interacting quantum fluids [1–5]. Utilizing a collisional (Feshbach) resonance, a bias magnetic field readily tunes interactions between spin-up and spin-down atoms from noninteracting to strongly repulsive or strongly attractive [6,7]. Several ground-breaking measurements have focused on the equilibrium thermodynamic properties [8–12]. However, systematic study of interaction-dependent hydrodynamic transport coefficients poses new challenges. Measurement of the shear viscosity is of particular interest in recent predictions [13–18] and in the context of a "perfect" fluid conjecture [19], derived using holographic duality methods [5]. The conjecture states that for a broad class of (conformal) strongly interacting quantum fields, the ratio of the shear viscosity η to the entropy density s has a universal minimum, $\eta/s \geq \hbar/(4\pi k_B)$ [19]. Recent measurements of the shear viscosity for a resonantly interacting Fermi gas [20,21] yield a minimum η/s ratio just 4.5 times the lower bound, comparable to that of a quark-gluon plasma [5]. Whether the shear viscosity of a Fermi gas (or the η/s ratio) is minimized at resonance or at a finite scattering length is an open question.

In this Letter, we describe a measurement of the shear viscosity η in an expanding Fermi gas as a function of the interaction strength and energy near a broad Feshbach resonance [6,7]. The shear viscosity is determined with high sensitivity by releasing the cloud from a cigar-shaped optical trap with an elliptical (1:2.7) transverse profile and measuring the transverse aspect ratio as a function of time after release [22]. The interaction strength is characterized by the dimensionless parameter $1/(k_{FI}a)$, where a is the s-wave scattering length and k_{FI} is the Fermi wave vector of an ideal gas at the trap center. First, we determine the shear viscosity at resonance, where $1/(k_{FI}a) = 0$, and then we determine the correction to the shear viscosity as a function of $1/(k_{FI}a)$. In kinetic theory, the correction term is expected to scale as $1/(k_{FI}a)^2$ [23]. However, for a given energy, we find there is an additional linear dependence on $1/(k_{FI}a)$ that results in a shift of the minimum viscosity.

For the experiments, we employ a Fermi gas of ^{6}Li atoms in a 50-50 mixture of the two lowest hyperfine states, which is confined in a cigar-shaped optical trap with aspect ratios $x:y:z = 1:2.7:33$. The cloud is tuned near a broad Feshbach resonance and cooled by evaporation [1]. After evaporative cooling, the interaction strength is adjusted by tuning the bias magnetic field. Then the optical trap is extinguished and the cloud radii are measured as a function of time after release in all three dimensions, using two simultaneous probe pulses interacting with different spin states to obtain independent absorption images on two CCD cameras [22].

We define a general, scattering-length-independent, energy scale $\tilde{E}$ for the trapped cloud by

$$\tilde{E} \equiv \frac{3}{N}\int d^3\mathbf{r}\, p_0 = \langle \mathbf{r}\cdot\nabla U\rangle_0. \tag{1}$$

Here, p_0 is the equilibrium pressure and $\tilde{E}$ is then three times the grand potential per particle [24]. The form on the right follows from force balance, $\nabla p_0 + n_0\nabla U = 0$, with n_0 the equilibrium density. $\tilde{E}$ is given by the trap average $\langle \mathbf{r}\cdot\nabla U\rangle_0 \equiv (1/N)\int d^3\mathbf{r}\, n_0(\mathbf{r})\mathbf{r}\cdot\nabla U$. For the measured trap parameters, given below, $\tilde{E}$ is then determined by the measured spatial profile of the trapped cloud [25]. Hence, by fixing $\tilde{E}$, we fix the average density for our measurements of viscosity at different interaction strengths.

The total trapping potential $U = U_{\rm opt} + U_{\rm mag}$ contains an optical part $U_{\rm opt}$ and a magnetic part $U_{\rm mag}$, arising from curvature in the bias magnetic field. For the optical potential, we find $\omega_x = 2\pi\times 2210(4)$, $\omega_y = 2\pi\times 830(2)$, and $\omega_{z\rm opt} = 2\pi\times 60.6(0.4)$ Hz. The additional magnetic potential $U_{\rm mag} = (1/2)m\omega_{\rm mag}^2(y^2 + z^2 - 2x^2)$, where m is the ^{6}Li mass and $\omega_{\rm mag} = 2\pi\times 21.5(0.25)\sqrt{B/834}$ Hz is the oscillation frequency of the cloud along the y axis, which is measured at 834 G with $U_{\rm opt} = 0$. For later use,

we define the ideal gas Fermi energy $E_F \equiv (3N)^{1/3}\hbar\bar{\omega}$, and the corresponding wave vector $k_{FI} = (2mE_F/\hbar^2)^{1/2}$, where N is the total number of atoms, which is typically 2×10^5 and $\bar{\omega} = (\omega_x\omega_y\omega_z)^{1/3}$ with $\omega_z = (\omega_{z\mathrm{opt}}^2 + \omega_{\mathrm{mag}}^2)^{1/2}$.

After release from the cigar-shaped trap, the transverse aspect ratio of the cloud exhibits elliptic flow in the x-y plane, indicating hydrodynamic expansion [22]. The shear viscosity pressure tensor slows the flow in the initially narrow, rapidly expanding, x direction and transfers energy to the more slowly expanding y direction. For a fixed time after release, the transverse aspect ratio σ_x/σ_y then decreases with increasing shear viscosity. In contrast to elliptic flow measurements employing the axial z direction, which expands slowly, the relatively high frequencies ω_x and ω_y assure that σ_x/σ_y saturates on a rapid time scale, where the expanded cloud images still have a high signal to background ratio, and reduces sensitivity to the magnetic potential.

The shear viscosity is given in natural units of $\hbar n$ by $\eta \equiv \alpha_S \hbar n$, where n is the density and α_S is a dimensionless shear viscosity coefficient [20]. The transverse aspect ratio data are fit using a hydrodynamic model, described below, to determine the *cloud-averaged* shear viscosity coefficient $\langle\alpha_S\rangle$, where

$$\langle\alpha_S\rangle \equiv \frac{1}{N\hbar}\int d^3\mathbf{r}\,\eta = \frac{1}{N}\int d^3\mathbf{r}\,n\alpha_S. \tag{2}$$

At finite scattering length, $\langle\alpha_S\rangle$ is generally time dependent, as discussed further below.

For our experiments below resonance, at low temperatures, a BEC would exist, and a two-fluid description would be required. To consistently compare our measurements of shear viscosity throughout the resonance region, we therefore work in the normal fluid regime, avoiding complications arising from two-fluid behavior that is not observed for the conditions of our experiments. Further, we estimate that the ratio of the collisional mean free path to the cloud size (the Knudsen number) is small for both the molecular and atomic components [25–27]. Hence, we determine the trap-averaged shear viscosity coefficients by fitting a hydrodynamic theory for a single component fluid.

For a single component fluid [25,28], the velocity field $\mathbf{v}(\mathbf{r}, t)$ obeys the Navier-Stokes equation [29], which includes the scalar pressure p, the trap potential U, and, generally,the shear and bulk viscosities [25]. With current conservation, we obtain exact evolution equations [30] for the mean square cloud sizes $\langle x_i^2\rangle$, $i = x, y, z$,

$$\frac{d^2}{dt^2}\frac{m\langle x_i^2\rangle}{2} = \frac{1}{N}\int d^3\mathbf{r}\,p + m\langle v_i^2\rangle - \langle x_i\partial_i U\rangle - \hbar\langle\alpha_S\sigma_{ii}\rangle, \tag{3}$$

where $\langle\ldots\rangle$ denotes an average over the cloud density, as in Eq. (2), and $\sigma_{ij} = \partial v_i/\partial x_j + \partial v_j/\partial x_i - 2\delta_{ij}\nabla\cdot\mathbf{v}/3$.

We see that the pressure p in Eq. (3) arises only in a volume integral, which we determine using energy conservation. After release of the cloud, when U is temporally constant, we have [25],

$$\frac{d}{dt}\int d^3\mathbf{r}\,\mathcal{E} + \int d^3\mathbf{r}\,(\nabla\cdot\mathbf{v})p = \dot{Q}, \tag{4}$$

where $\mathcal{E}$ is the energy density and $\dot{Q}$ is the total heating rate arising from the viscous forces [25]. Equation (4) is used to find $(1/N)\int d^3\mathbf{r}p$ by eliminating $\mathcal{E}$, using $p = (2/3)\mathcal{E} + \Delta p$, where Δp is the predicted conformal symmetry breaking pressure, which vanishes at resonance [22,31]. Note that the measured $\tilde{E}$ in Eq. (1) determines the initial condition, $(1/N)\int d^3\mathbf{r}p_0$.

To solve Eqs. (3) and (4), we use a scaling approximation, which has been shown to be very accurate using numerical viscous hydrodynamics [32]. Then, $\langle x_i^2\rangle = \langle x_i^2\rangle_0 b_i^2(t)$ and $\langle v_i^2\rangle = \langle x_i^2\rangle_0 \dot{b}_i^2(t)$, where b_x, b_y, b_z are the expansion scale factors and $\langle x_i^2\rangle_0$ is the measured mean square size just after release. In the scaling approximation, $v_i = x_i\dot{b}_i/b_i$ and $\nabla\cdot\mathbf{v} = \dot{\Gamma}/\Gamma$, where $\Gamma \equiv b_x b_y b_z$ is the volume scale factor and Γ and σ_{ii} are functions only of the time. The scale factors obey

$$\ddot{b}_i = \frac{\overline{\omega_i^2}}{\Gamma^{2/3}b_i}[1 + C(t)] - \frac{\hbar\langle\alpha_S\rangle\sigma_{ii}}{m\langle x_i^2\rangle_0 b_i} - \omega_{\mathrm{imag}}^2 b_i. \tag{5}$$

In Eq. (5), we define $\overline{\omega_i^2} \equiv \tilde{E}/(3m\langle x_i^2\rangle_0)$ for an arbitrary trapping potential, which need not be harmonic [25] and $\omega_{y\mathrm{mag}}^2 = \omega_{z\mathrm{mag}}^2 = \omega_{\mathrm{mag}}^2$ and $\omega_{x\mathrm{mag}}^2 = -2\omega_{\mathrm{mag}}^2$ (repulsive), with ω_{mag} defined above.

The coefficient $C(t) = C_Q(t) + C_{\Delta p}(t)$ in Eq. (5) includes two effects exactly (within the scaling approximation): C_Q is the fractional increase in the volume integrated pressure arising from viscous heating, which is determined by $\dot{Q}$ [25]. $C_{\Delta p}(t)$ describes the corresponding fractional change for a given conformal symmetry breaking pressure change $\Delta p(t)$. For the transverse aspect ratio, σ_x/σ_y, we find that C_Q is important, but that $C_{\Delta p}$ has a negligible effect [25].

The shear viscosity coefficient $\langle\alpha_S\rangle$ is measured by using Eq. (5) to fit the data for the transverse aspect ratio $\sigma_x/\sigma_y = \omega_y b_x/(\omega_x b_y)$ as a function of time after release, while self consistently determining $\tilde{E}/E_F$ from the measured cloud sizes $\sigma_x, \sigma_y, \sigma_z$, and N. At resonance, where the scattering length a diverges and $1/(k_{FI}a) = 0$, α_S can be a function only of the local reduced temperature $\theta \propto T/n^{2/3}$. As the viscosity makes a small perturbation to the flow, we approximate the temperature within the viscosity coefficient in zeroth order; i.e., we assume that the temperature evolves adiabatically during the expansion after the optical trap is abruptly extinguished. Then $T \propto n^{2/3}$, so that the local θ remains fixed at its initial value. In this case, $\langle\alpha_S\rangle \equiv \langle\alpha_S\rangle_0$ is temporally constant as the cloud expands; i.e., it is equal to the trap-averaged initial value with $n \to n_0$.

We determine $\langle\alpha_S\rangle$ both on resonance, where $\langle\alpha_S\rangle = \langle\alpha_S\rangle_0$ is temporally constant, and at finite $1/(k_{FI}a)$, initially ignoring the time dependence arising from the finite scattering length, which we include later in Eq. (6). Figure 1 shows the difference $\Delta\langle\alpha_S\rangle = \langle\alpha_S\rangle - \langle\alpha_S\rangle_0$ between the $\langle\alpha_S\rangle$ determined at finite $1/(k_{FI}a)$ and the resonant value $\langle\alpha_S\rangle_0$. We determine $\langle\alpha_S\rangle_0$ from a polynomial fit to the resonant shear viscosity as a function of $\tilde{E}/E_F$ [25].

We find that the minimum in shear viscosity occurs on the BEC side of resonance, Fig. 1(c). Further, we note that the $\Delta\langle\alpha_S\rangle$ depends strongly on the magnitude and sign of the interaction strength $1/(k_{FI}a)$. Generally, on the BEC side of resonance $1/(k_{FI}a) > 0$, we find that $\Delta\langle\alpha_S\rangle$ increases with increasing energy, which may arise from a corresponding decrease in the dimer fraction, as discussed further below. On the BCS side of resonance $1/(k_{FI}a) < 0$, $\Delta\langle\alpha_S\rangle$ decreases with increasing energy, which may arise from reduced Pauli blocking; i.e., the collision rate increases with temperature in the degenerate regime. Clearly, a simple quadratic dependence on the interaction strength is insufficient to encompass all the observed behavior of $\Delta\langle\alpha_S\rangle$.

In order to investigate further, we fit a linear energy dependence to $\Delta\langle\alpha_S\rangle$ for each interaction strength $1/(k_{FI}a)$ as shown in Fig. 1. In Fig. 2, $\Delta\langle\alpha_S\rangle$ is plotted as a function of $1/(k_{FI}a)$ for a fixed energy $\tilde{E}/E_F = 1$. We see a nominally parabolic dependence on $1/(k_{FI}a)$, with the minimum clearly shifted toward the BEC side of resonance. Setting $\Delta\langle\alpha_S\rangle = \tilde{c}_0 + \tilde{c}_1/(k_{FI}a) + \tilde{c}_2/(k_{FI}a)^2$, we fit the data shown in Fig. 1 excluding the two extreme $1/(k_{FI}a)$ points where a simple perturbation expansion in $1/(k_{FI}a)$ is likely to break down. We find $\tilde{c}_0 = 0.0$, $\tilde{c}_1 = -1.7$, and $\tilde{c}_2 = 4.8$. Recall that we have ignored the expansion time dependence arising from the finite scattering length. Therefore, we can only draw qualitative conclusions from our fit to $\Delta\langle\alpha_S\rangle$ versus $1/(k_{FI}a)$.

We now obtain quantitative results for the dependence of the shear viscosity on $1/(k_{FI}a)$ by including the explicit time dependence of the shear viscosity coefficients and refitting the data. Using dimensional analysis, the leading-order scattering-length-dependent terms in local shear viscosity take the forms $\hbar n f_1(\theta)/(k_F a)$ $\hbar n f_2(\theta)/(k_F a)^2$, where $f_{1,2}(\theta)$ are dimensionless functions of the reduced temperature. Then, in the scaling approximation described above, the density $n \propto k_F^3$ decreases by the volume scale factor Γ as the cloud expands, so that $1/k_F \propto \Gamma^{1/3}(t)$. For the viscosity coefficients, we again approximate the temperature to zeroth order as evolving adiabatically, so that $f_{1,2}(\theta)$ are temporally constant. Averaging over the cloud volume, as in Eq. (2), we then obtain the general form for the time-dependent cloud-averaged viscosity coefficient,

$$\langle\alpha_S\rangle = \langle\alpha_S\rangle_0 + c_1\frac{\Gamma^{1/3}(t)}{k_{FI}a} + c_2\frac{\Gamma^{2/3}(t)}{(k_{FI}a)^2}. \qquad (6)$$

In the spirit of a perturbation expansion in $1/(k_{FI}a)$ about resonance at fixed $\tilde{E}$, the first term is taken to be the shear

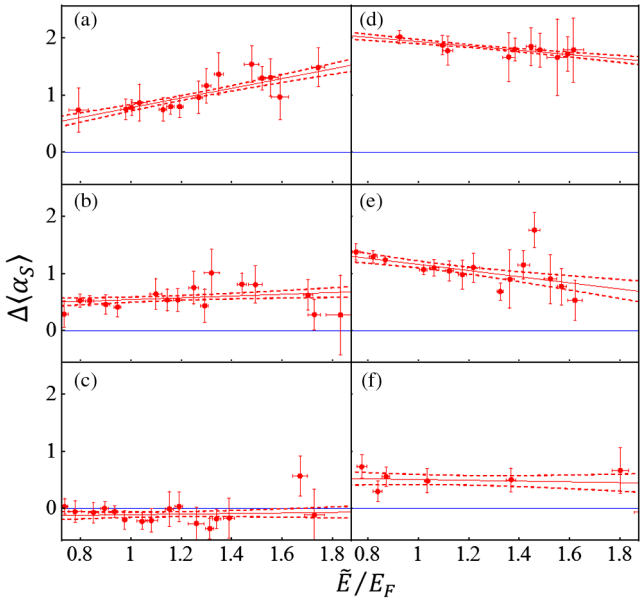

FIG. 1 (color online). Difference in shear viscosity on and off resonance, $\Delta\langle\alpha_S\rangle$, versus energy $\tilde{E}/E_F$ and interaction strength $1/(k_{FI}a)$. On the BEC side of resonance (left column), $1/(k_{FI}a) =$ (a) 0.83(6), (b) 0.55(5), and (c) 0.25(3). On the BCS side of resonance (right column) $1/(k_{FI}a) =$ (d) −0.61(1), (e) −0.34(1), and (f) −0.16(3). Red line denotes linear fit to $\Delta\langle\alpha_S\rangle(\tilde{E})$. Dotted red lines show 1-σ confidence interval. Blue (solid) lines show the resonant shear viscosity $\langle\alpha_S\rangle_0$, (which denotes zero by construction).

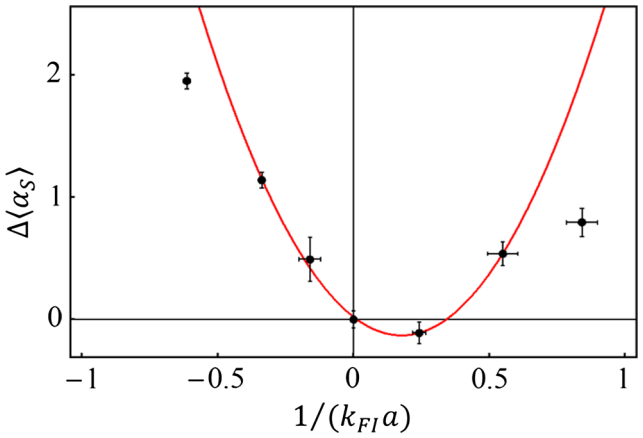

FIG. 2 (color online). Difference in shear viscosity on and off resonance, $\Delta\langle\alpha_S\rangle$, versus interaction strength $1/(k_{FI}a)$ at an energy of $\tilde{E}/E_F = 1$. Black circles represent $\Delta\langle\alpha_S\rangle$ obtained from the linear fits in Fig. 1. Vertical error bars are the 1–σ confidence interval of the fits. The red (parabolic curve) is the best fit of $\tilde{c}_0 + \tilde{c}_1/(k_{FI}a) + \tilde{c}_2/(k_{FI}a)^2$ to the data with $\tilde{c}_0 = 0.0$, $\tilde{c}_1 = -1.7$, and $\tilde{c}_2 = 4.8$. From the fit, the minimum occurs at $1/(k_F a) = 0.18$.

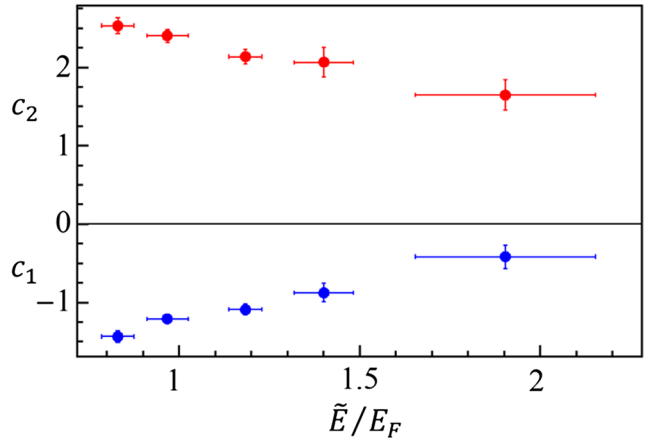

FIG. 3 (color online). Off resonant shear viscosity coefficients c_1 and c_2 from Eq. (6), $\langle\alpha_S\rangle_0 + c_1\Gamma_1^{1/3}(t)/(k_{FI}a) + c_2\Gamma_1^{2/3}(t)/(k_{FI}a)^2$, obtained by integrating Eq. (5) and globally minimizing χ^2 for aspect ratio data within a range of energies and interactions strengths. Red (upper) circles are c_2 versus energy. Blue (lower) circles are c_1 versus energy.

viscosity coefficient at resonance, which is time independent and determined versus $\tilde{E}$, as described above.

We globally fit the data over discrete energy ranges and limit the range of interaction strength to $-0.5 < 1/(k_{Fi}a) < 0.7$. This is accomplished by integrating Eq. (5), using Eq. (6). As $\langle\alpha_S\rangle_0$ is known as a function of $\tilde{E}$, c_1 and c_2 are used as fit parameters, determined by a χ^2 fit to the aspect ratio data. The results are shown in Fig. 3.

For an energy range of $0.9 < \tilde{E}/E_F < 1.1$, 71 points are included in the two parameter fit with an average energy of $\tilde{E}/E_F = 0.97(6)$. We obtain a normalized $\chi^2 = 1.1$, with $c_1 = -1.22(5)$ and $c_2 = 2.43(9)$. Equation (6) then yields a minimum in the initial (in-trap) shear viscosity at $1/(k_{FI}a) = -c_1/(2c_2) = 0.25$. For an energy of $\tilde{E}/E_F = 0.97$, the polynomial fit for the resonant gas gives a shear viscosity of $\langle\alpha_S\rangle_0 = 1.10$, so that at $t = 0$, $\langle\alpha_S\rangle_{\min} = \langle\alpha_S\rangle_0 - c_1^2/(4c_2) = 0.95$. Note that the smaller values of the in-trap $c_{1,2}$ compared to $\tilde{c}_{1,2}$ are consistent with the time-dependent factors in Eq. (6), since $\Gamma(t)$ increases from unity as the cloud expands. Complete results can be found in Ref. [25].

The shift of the minimum shear viscosity toward the BEC side of resonance may be explained by an enhancement in the bosonic degrees of freedom [15], such as preformed atom pairs or dimer molecules. These bosonic degrees of freedom would suppress Pauli blocking and increase the effective scattering rate [13]. In addition, the collisional cross section for dimer-atom scattering is larger than that for atom-atom scattering [27]. Therefore, since the shear viscosity scales inversely with the scattering rate, one would expect the observed decrease on the BEC side. We note also that $\langle\alpha_S\rangle$ is well below the parabolic fit at the two extreme points $1/(k_{FI}a) = 0.83$ and $1/(k_{FI}a) = -0.61$. This may be a consequence of a divergence of the expansion in powers $1/(k_{FI}a)$, but may also be the result of a larger dimer fraction on the BEC side of resonance. We observe also that the location of the minimum in the shear viscosity, $-c_1/(2c_2)$, moves toward resonance with increasing energy [25], indicating that the $\langle\alpha_S\rangle$ may scale quadratically with $1/(k_{FI}a)$ at higher temperatures, as predicted [23].

This research is supported by the Physics Division of the National Science Foundation (quantum transport in strongly interacting Fermi gases PHY-1067873), the Division of Materials Science and Engineering, the Office of Basic Energy Sciences, Office of Science, U.S. Department of Energy (thermodynamics in strongly correlated Fermi gases DE-SC0008646), the Physics Divisions of the Army Research Office (strongly interacting Fermi gases in reduced dimensions W911NF-11-1-0420) and the Air Force Office of Scientific Research (nonequilibrium Fermi gases FA9550-13-1-0041). The authors are pleased to acknowledge K. Dusling and T. Schäfer, North Carolina State University, for stimulating conversations.

[1] K. M. O'Hara, S. L. Hemmer, M. E. Gehm, S. R. Granade, and J. E. Thomas, Science **298**, 2179 (2002).
[2] S. Giorgini, L. P. Pitaevskii, and S. Stringari, Rev. Mod. Phys. **80**, 1215 (2008).
[3] W. Ketterle and M. W. Zwierlein, Rivista del Nuovo Cimento **31**, 247 (2008).
[4] I. Bloch, J. Dalibard, and W. Zwerger, Rev. Mod. Phys. **80**, 885 (2008).
[5] A. Adams, L. D. Carr, T. Schäfer, P. Steinberg, and J. E. Thomas, New J. Phys. **14**, 115009 (2012).
[6] M. Bartenstein *et al.*, Phys. Rev. Lett. **94**, 103201 (2005).
[7] G. Zürn, T. Lompe, A. N. Wenz, S. Jochim, P. S. Julienne, and J. M. Hutson, Phys. Rev. Lett. **110**, 135301 (2013).
[8] L. Luo, B. Clancy, J. Joseph, J. Kinast, and J. E. Thomas, Phys. Rev. Lett. **98**, 080402 (2007).
[9] L. Luo and J. E. Thomas, J. Low Temp. Phys. **154**, 1 (2009).
[10] M. Horikoshi, S. Najajima, M. Ueda, and T. Mukaiyama, Science **327**, 442 (2010).
[11] S. Nascimbène, N. Navon, K. J. Jiang, F. Chevy, and C. Salomon, Nature (London) **463**, 1057 (2010).
[12] M. Ku, A. T. Sommer, L. W. Cheuk, and M. W. Zwierlein, Science **335**, 563 (2012).
[13] G. M. Bruun and H. Smith, Phys. Rev. A **75**, 043612 (2007).
[14] E. Taylor and M. Randeria, Phys. Rev. A **81**, 053610 (2010).
[15] H. Guo, D. Wulin, C.-C. Chien, and K. Levin, Phys. Rev. Lett. **107**, 020403 (2011).
[16] T. Enss, R. Haussmann, and W. Zwerger, Ann. Phys. (Amsterdam) **326**, 770 (2011).
[17] G. Wlazłowski, P. Magierski, and J. E. Drut, Phys. Rev. Lett. **109**, 020406 (2012).
[18] G. Wlazłowski, P. Magierski, A. Bulgac, and K. J. Roche, Phys. Rev. A **88**, 013639 (2013).

[19] P. K. Kovtun, D. T. Son, and A. O. Starinets, Phys. Rev. Lett. **94**, 111601 (2005).
[20] C. Cao, E. Elliott, J. Joseph, H. Wu, J. Petricka, T. Schäfer, and J. E. Thomas, Science **331**, 58 (2011).
[21] C. Cao, E. Elliott, H. Wu, and J. E. Thomas, New J. Phys. **13**, 075007 (2011).
[22] E. Elliott, J. A. Joseph, and J. E. Thomas, Phys. Rev. Lett. **112**, 040405 (2014).
[23] G. M. Bruun and H. Smith, Phys. Rev. A **72**, 043605 (2005).
[24] For the resonantly interacting gas, where $p = 2\mathcal{E}/3$ with $\mathcal{E}$ the local energy density [31], $\tilde{E}/2$ is just the internal energy per particle [33]. At resonance, the total energy is then $E = \langle U \rangle_0 + \tilde{E}/2$, with $\langle U \rangle_0 \equiv (1/N) \int d^3\mathbf{r} n_0(\mathbf{r}) U(\mathbf{r})$ [9].
[25] See Supplemental Material at http://link.aps.org/supplemental/10.1103/PhysRevLett.113.020406 for derivation of the hydrodynamic equations, justification of the single-fluid description, and data analysis methods.
[26] D. S. Petrov, C. Salomon, and G. V. Shlyapnikov, Phys. Rev. Lett. **93**, 090404 (2004).
[27] D. S. Petrov, C. Salomon, and G. V. Shlyapnikov, Phys. Rev. A **71**, 012708 (2005).
[28] Y.-H. Hou, L. P. Pitaevskii, and S. Stringari, Phys. Rev. A **87**, 033620 (2013).
[29] L. D. Landau and E. M. Lifshitz, *Fluid Mechanics* (Elsevier, New York, 1987).
[30] We ignore the bulk viscosity, which is found to be much smaller than shear viscosity [22,25].
[31] T.-L. Ho, Phys. Rev. Lett. **92**, 090402 (2004).
[32] T. Schäfer, Phys. Rev. A **82**, 063629 (2010).
[33] J. E. Thomas, J. Kinast, and A. Turlapov, Phys. Rev. Lett. **95**, 120402 (2005).